AIMS Mathematics, 9(7): 17025–17038.
DOI: 10.3934/math.2024826
Received: 13 March 2024
Revised: 22 April 2024
Accepted: 09 May 2024
Published: 16 May 2024

https://www.aimspress.com/journal/Math

Research article

Bifurcation and chaos in simple discontinuous systems separated by a hypersurface

Hany A. Hosham[1,*] **and Thoraya N. Alharthi** [2]

[1] Department of Mathematics, Faculty of Science, Taibah University, Yanbu, 41911, Saudi Arabia
[2] Department of Mathematics, College of Science, University of Bisha, P.O. Box 551, Bisha 61922, Saudi Arabia

* **Correspondence:** Email: ybakit@taibahu.edu.sa.

Abstract: This research focuses on a mathematical examination of a path to sliding period doubling and chaotic behaviour for a novel limited discontinuous systems of dimension three separated by a nonlinear hypersurface. The switching system is composed of dissipative subsystems, one of which is a linear systems, and the other is not linked with equilibria. The non-linear sliding surface is designed to improve transient response for these subsystems. A Poincaré return map is created that accounts for the existence of the hypersurface, completely describing each individual sliding period-doubling orbits that route to the sliding chaotic attractor. Through a rigorous analysis, we show that the presence of a nonlinear sliding surface and a set of such hidden trajectories leads to novel bifurcation scenarios. The proposed system exhibits period-m orbits as well as chaos, including partially hidden and sliding trajectories. The results are numerically verified through path-following techniques for discontinuous dynamical systems.

Keywords: discontinuous systems; bifurcations; period-doubling; sliding mode; chaos
Mathematics Subject Classification: 34A36, 34D23, 37G15, 34H10

1. Introduction

This article analyses a special type of dynamical system described by vector fields with jump discontinuities along specified nonlinear hypersurfaces of the Euclidean space. We refer the reader to [1–7] as a general references covering various concepts, theories, methods, applications and challenges. Several real-world problems frequently lead to discontinuous systems, such as biological systems, which are expressed by switching event functions; see [8–11]. Recently, there has been a lot of interest in sliding mode control in mechanical systems with dry friction, where the objective of a control system is to reach a specific sliding manifold in a finite time [12].

According to these diverse studies, the development of novel mathematical approaches for the analysis of discontinuous systems is interesting, but complicated due to the classical methods such as, Lyapunov-Schmidt and center manifold theory, are no longer directly applicable to dealing with an abrupt change in the governing vector fields. Indeed, significant progress has been made in developing the classical methods of bifurcations to deal with the classification and characterization of, singularities, attractors, and hidden chaotic attractors for discontinuous systems [1, 13–15]. Although there have been successful studies on calculating the Lyapunov exponent for certain types of discontinuous dynamical systems, such as [16–18], there are still challenges to effectively implementing it. The main issue is that there is no generalized algorithm for effectively coordinating the root finding of indicator functions in discontinuous systems with multiple sudden changes and repeated reordering for linearized (variational) equations. The method of the Poincaré map, which includes invariance and attraction, has produced numerous interesting findings on bifurcation and periodic orbits with a single line of discontinuity; see, for example, [19].

Smooth dynamic systems, such as continuous flow or maps, exhibit period-doubling bifurcation as a route to chaos [20]. As well, many methods, such as the Lyapunov exponent method, are used directly to predict chaotic behavior. However, the presence of nonsmooth nonlinearities in discontinuous systems poses various difficulties, therefore requiring the development of both analytical and numerical approaches to effectively address these characteristics.

In the continuous dynamical system, the hidden attractor is generated by a very small basin of attraction, which may oscillate between the two scenarios of having no equilibrium or having stable equilibria [21]. In the area of discontinuous dynamical systems, it was recently shown in [22, 23] that a planar linear non-smooth system with no equilibria in each subsystem, whether real or virtual, can still exhibit at least one limit cycle. In our current study, the hidden dynamics of the proposed 3-dimensional discontinuous system is related to the fact that only one subsystem in the whole system lacks an equilibrium point.

The primary contribution of this work is to present a novel, simple dynamical system capable of involving complicated bifurcation phenomena. Our main objective is to investigate the situation of intersections of large dimensions and associated sliding modes. The proposed system's dynamics are easily explained and studied by generalizing the Poincaré map, which is created by identifying explicit, exact solutions for each subsystem. The linear subsystem has only a unique equilibrium point, whereas the other subsystem lacks an equilibrium point and therefore may exhibit a hidden attractor. It should be noted here that the hidden dynamic of a sliding motion is quite different and is described by the smooth transition from ingoing to outgoing solution paths, which occurs instantly in the jump discontinuity of the flow. Analyzing this type of hidden dynamics is significantly complex, and achieving a comprehensive classification is not yet feasible. In this context, some interesting categories have been presented [3, 5]. We use analytical and numerical methods to investigate flow behavior along a nonlinear sliding surface and hidden trajectory. We will demonstrate that the proposed system displays period-m orbits, as well as chaos, which includes partially hidden and sliding trajectories.

The paper is structured as follows: Section 2 introduces the fundamental principles of discontinuous differential systems and switching behavior rules. Section 3 introduces the discontinuous system and presents its analytical solutions. Moreover, a Poincaré return map is developed to establish the criteria for predicting period-doubling and chaos. In Section 4, we show that the proposed system has rich dynamics, including periodic, multi-periodic, and chaotic behavior involving sliding modes. Section 5

concludes with a summary of the obtained results.

2. Fundamental concept

Definition 1. *Mathematically, a hypersurface is codimension one subset* $\tilde{\Sigma}$ *of in the Euclidean space* $\mathbb{R}^n$*, i.e.,* $\tilde{\Sigma} := \{\mathcal{X} \in \mathbb{R}^n \mid H(\mathcal{X}, \alpha) = 0$*, such that* $H : \mathbb{R}^n \longrightarrow \mathbb{R}^d, d < n$ *is sufficiently differentiable, and the hypersurface intersects transversally.*

For example, in this paper, we examine the limit period-m orbits, cycles, and chaos in two discontinuous differential systems separated by the hypersurface, which is represented by the cubic function as:

$$\tilde{\Sigma} := \{\mathcal{X} \in \mathbb{R}^3 \mid H(\mathcal{X}, \alpha) = \gamma_1 z + \gamma_2 y + \gamma_3 x^3 = 0\}. \tag{2.1}$$

Let us consider the vector $\mathcal{X} \in \mathbb{R}^n$, whose time dependence is defined by the vector fields $F_i : \mathbb{R}^n \longrightarrow \mathbb{R}^n$, i=1,2, such that

$$\dot{\mathcal{X}} = \begin{cases} F_1(\mathcal{X}, \alpha), & H(\mathcal{X}, \alpha) < 0, \\ F_2(\mathcal{X}, \alpha), & H(\mathcal{X}, \alpha) > 0, \end{cases} \tag{2.2}$$

where the phase space divides into two bounded domains D_i separated by a hypersurface $\tilde{\Sigma} = \{\mathcal{X} \in \mathbb{R}^n \mid H(\mathcal{X}, \alpha) = 0\}$ where $H(\mathcal{X}, \alpha)$ is a continuous function and $\alpha \in \mathbb{R}^d$. The functions $F_i, i = 1, 2$ are uniformly smooth functions ($F_i \in \mathbb{C}^k(\tilde{\Sigma}, \mathbb{R}^n),\ k \geq 1$), and satisfy the fundamental matrix systems

$$\dot{\Phi}(\mathcal{X}, t) = F_i(\Phi(\mathcal{X}, t)), \quad \Phi(\mathcal{X}, 0) = I.$$

The identity matrix I has the same order as the number of state variables. The following principles may be required to characterize the interaction on the discontinuity surface $\tilde{\Sigma}$, due to the flow of (2.2) must be uniquely described in forward time. Let $\varrho(\mathcal{X}, \alpha) = (n^T(\mathcal{X}, \alpha)F_1(\mathcal{X}, \alpha)).(n^T(\mathcal{X}, \alpha)F_2(\mathcal{X}, \alpha))$, where $n(\mathcal{X}, \alpha)$ is a normal vector to this surface $H(\mathcal{X}, \alpha)$. Consequently, the discontinuity surface $\tilde{\Sigma}$ can be partitioned as follows:

- Crossing region $\tilde{\Sigma}^c = \{\mathcal{X} \in \tilde{\Sigma} \mid \varrho(\mathcal{X}) > 0\}$, more specifically $\tilde{\Sigma}^c = \tilde{\Sigma}^c_- \cup \tilde{\Sigma}^c_+$ such that $\tilde{\Sigma}^c_\pm = \{\mathcal{X} \in \tilde{\Sigma}^c \mid \pm n^T(\mathcal{X}, \alpha)F_1(\mathcal{X}, \alpha) > 0\}$.
- Sliding region $\tilde{\Sigma}^s = \{\mathcal{X} \in \tilde{\Sigma} \mid \varrho(\mathcal{X}) \leq 0\}$, which in turn is divided into attractive region $\tilde{\Sigma}^s_- = \{\mathcal{X} \in \tilde{\Sigma}^s \mid n^T(\mathcal{X}, \alpha)F_1(\mathcal{X}, \alpha) > 0\}$, and escaping region $\tilde{\Sigma}^s_+ = \{\mathcal{X} \in \tilde{\Sigma}^s \mid n^T(\mathcal{X}, \alpha)F_2(\mathcal{X}, \alpha) > 0\}$.
- Boundaries between sliding and crossing modes are defined as: $\tilde{\Sigma}^0_- = \{\mathcal{X} \in \tilde{\Sigma} \mid n^T(\mathcal{X}, \alpha)F_2(\mathcal{X}, \alpha) = 0\}$, $\tilde{\Sigma}^0_+ = \{\mathcal{X} \in \tilde{\Sigma} \mid n^T(\mathcal{X}, \alpha)F_1(\mathcal{X}, \alpha) = 0\}$.

Observe that $\tilde{\Sigma}$ represents the disjoint union $\tilde{\Sigma}^c \cup \tilde{\Sigma}^0_\pm \cup \tilde{\Sigma}^s$.
The sliding flows on $\tilde{\Sigma}^s$ are defined by the Filippov convex combination as:

$$\dot{\mathcal{X}} = F_3(\mathcal{X}, \alpha) = \frac{P(\mathcal{X}, \alpha)}{Q(\mathcal{X}, \alpha)} \tag{2.3}$$

where $P(\mathcal{X}, \alpha) = n^T(\mathcal{X}, \alpha)F_2(\mathcal{X}, \alpha) \cdot F_1(\mathcal{X}, \alpha) - n^T(\mathcal{X}, \alpha)F_1(\mathcal{X}, \alpha) \cdot F_2(\mathcal{X}, \alpha)$ and $Q(\mathcal{X}, \alpha) = n^T(\mathcal{X}, \alpha)(F_2(\mathcal{X}, \alpha) - F_1(\mathcal{X}, \alpha))$. Flow can become tangent to the boundary of a discontinuity surface $\tilde{\Sigma}$ from either side; $\mathcal{X} \in \tilde{\Sigma}^0_-$ or $\mathcal{X} \in \tilde{\Sigma}^0_+$ (i.e., $n^T(\mathcal{X}, \alpha)F_1(\mathcal{X}, \alpha) = 0$ or $n^T(\mathcal{X}, \alpha)F_2(\mathcal{X}, \alpha) = 0$), resulting in a fold singularity. A two-fold singularity occurs if $\mathcal{X} \in \tilde{\Sigma}^0_- \cap \tilde{\Sigma}^0_+$ (i.e., $n^T(\mathcal{X}, \alpha)F_i(\mathcal{X}, \alpha) = 0, i = 1, 2$). A two-fold singularity creates unique and intricate phenomena in discontinuous systems; see [5, 24, 25].

3. Chaos in discontinuous systems characterized by non-smooth transitions

The Poincaré map is helpful for describing the bifurcation of non-smooth systems with varying parameters. It is worth noting that those Poincaré maps are discrete maps specified in dimension $n-1$, hence at this phase, result of Lie and Yorke "period three implies chaos" is not available [20, 26].

Let us identify a direction starting from the starting position $\mathcal{X}_0 \in \tilde{\Sigma}^c_-$ or $\mathcal{X}_0 \in \tilde{\Sigma}^c_+$ or $\mathcal{X}_0 \in \tilde{\Sigma}^s_-$ then the trajectory of solutions of systems $\dot{\mathcal{X}} = F_r(\mathcal{X}, \alpha)$ is denoted by $\Psi_r(T_r(\mathcal{X}), \mathcal{X}), r = 1, 2, 3$, receptively which are $\mathbb{C}^k, k \geq 1$. Assume that $\Psi_r(T_r(\mathcal{X}), \mathcal{X})$ reaches $\tilde{\Sigma}^c_{\mp}$, or $\tilde{\Sigma}^s_-$ (occurring, receptively) at the minimum return times $T_r(\mathcal{X})$. The return times $T_r(\mathcal{X})$ are found as the first positive solutions for the following systems:

$$T_r(\mathcal{X}) := \inf\{T > 0 \mid n^T(\mathcal{X})(\Psi_r(T(\mathcal{X}), \mathcal{X}) = 0\}, k = 1, 2, 3. \tag{3.1}$$

If these times exist, then we define the sub-maps as follows:

$$\begin{aligned} &\tilde{\mathcal{P}}_1(\mathcal{X}) : \tilde{\Sigma}^c_- \to \tilde{\Sigma}^c_+, \text{or } \tilde{\mathcal{P}}_1(\mathcal{X}) : \tilde{\Sigma}^c_- \to \tilde{\Sigma}^s_-, \\ &\tilde{\mathcal{P}}_2(\mathcal{X}) : \tilde{\Sigma}^c_+ \to \tilde{\Sigma}^c_-, \text{or } \tilde{\mathcal{P}}_2(\mathcal{X}) : \tilde{\Sigma}^c_+ \to \tilde{\Sigma}^s_-, \\ &\tilde{\mathcal{P}}_3(\mathcal{X}) : \tilde{\Sigma}^s_- \to \tilde{\Sigma}^c_-, \text{or } \tilde{\mathcal{P}}_3(\mathcal{X}) : \tilde{\Sigma}^s_- \to \tilde{\Sigma}^c_+. \end{aligned} \tag{3.2}$$

A generalized Poincaré map is defined as a composition of sub-maps $\tilde{\mathcal{P}}_i(\mathcal{X})$; for instance, in crossing mode, only the Poincaré map is given as

$$\tilde{\mathcal{P}}(\mathcal{X}) : \tilde{\Sigma}^c_- \to \tilde{\Sigma}^c_- = \tilde{\mathcal{P}}_1(\mathcal{X}) \circ \tilde{\mathcal{P}}_2(\mathcal{X}).$$

To predict the periodic orbit of our system (2.2), we consider the function

$$\delta(\mathcal{X}) : U \subset \tilde{\Sigma}^c_- \to \tilde{\Sigma}^c_- = \tilde{\mathcal{P}}(\mathcal{X}) - \mathcal{X} = 0.$$

If a sliding mode exists, $\tilde{\mathcal{P}}(\mathcal{X})$ is a composite of a sub-map $\tilde{\mathcal{P}}_3(\mathcal{X})$ and either $\tilde{\mathcal{P}}_1(\mathcal{X})$, $\tilde{\mathcal{P}}_2(\mathcal{X})$, or $\tilde{\mathcal{P}}_i(\mathcal{X}), i = 1, 2$, depending on the system trajectory behavior.

The following theorem indicates that the linearization of the Poincaré return map is used to predict the period-m orbit.

Theorem 1. *Crossing mode: Assume that $\mathcal{X} \in \tilde{\Sigma}^c_-$ and $\tilde{\mathcal{P}}^{(m)} : \tilde{\Sigma}^c_- \to \tilde{\Sigma}^c_-$, such that $\tilde{\mathcal{P}}^{(m)}(0) = 0$ and $\tilde{\mathcal{P}}^{(m)}(\bar{\mathcal{X}}) = \bar{\mathcal{X}}$. Then, the linearization of the Poincaré map is given by*

$$D_{\mathcal{X}}\tilde{\mathcal{P}}^{(m)} = \prod_{r=1}^{m} \tilde{S}_2^{(m+1-r)} \Phi_2^{(m+1-r)} \tilde{S}_1^{(m+1-r)} \Phi_1^{(m+1-r)}. \tag{3.3}$$

where $\tilde{S}_i, i = 1, 2$ are called transition matrices. Further, $\tilde{\mathcal{P}}^{(m)}(\bar{\mathcal{X}})\mathcal{X}_1(\bar{\mathcal{X}}) = \mathcal{X}_1(\bar{\mathcal{X}})$, and the attractivity of the period-m orbit is determined by the remaining $(n-2)$ eigenvalues of $D_{\mathcal{X}}\tilde{\mathcal{P}}^{(m)}$.

It should be mentioned that when $(m = 1)$, this theorem has been proved by [19, 27, 28], and when $(m \geq 1)$, and if $m = 2$ it has been proved by [29] and it is valid when considering a sliding mode for any arbitrary n-dimensional nonsmooth system.

It is well known that the continuous system $\dot{\mathcal{X}} = F(\mathcal{X}, \alpha)$ exhibits chaotic behavior if it is sensitive to the starting points of solutions and has an infinite number of unstable periodic trajectories with

different periods. Period-doubling bifurcation is a technique that has been used to cause chaos in many well-known systems, including the Lorenz and Chua systems. In one-dimensional discrete systems, however, the period doubling method was also used to generate chaotic behaviour. In this context, Lie and Yorke presented the result that "period three implies chaos" and applies to one-dimensional discrete systems [26]. But this approach is not available here due to the $\dim(\tilde{\mathcal{P}}) \geq 2$. Thus, we establish a theoretical approach to investigating the way to chaos for bounded nonsmooth systems of dimension three with switching surfaces that is defined as $H(\mathcal{X}, \alpha) = \gamma_1 z + \gamma_2 y + \gamma_3 x^3$. If $H(\mathcal{X}, \alpha) > 0$, one of the vector fields is linear and given as:

$$\dot{\mathcal{X}} = F_2(\mathcal{X}, \alpha) = \begin{pmatrix} \alpha_1 y \\ -\alpha_2 x \\ \alpha_3 z \end{pmatrix}. \tag{3.4}$$

It is obvious that the system $\dot{\mathcal{X}} = F_2(\mathcal{X}, \alpha)$ has only one non-hyperbolic equilibrium point at the origin, with three eigenvalues $\sigma_{1,2} = \pm i\beta, \sigma_3 = \alpha_3$, where $0 < \alpha_1\alpha_2 = \beta^2$. This system is dissipative if $\alpha_3 < 0$. In the situation where only the system $\dot{\mathcal{X}} = F_2(\mathcal{X}, \alpha)$ is defined in a smooth region, then the system has an invariant plane $z = 0$, and there is only one family of flat periodic orbits [2] located in the $(x, y)-$ plane with a constant time $t = 2\pi/\beta$, see Figure 1.

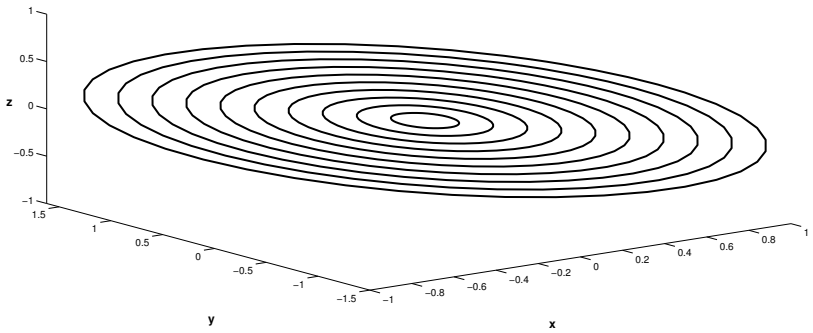

Figure 1. Family of flat periodic orbits located in the $(x, y)-$ plane with constant time $T = 2\pi/\beta$.

When a linear system interacts with a sliding surface, the trajectory may show chattering or frequent switching around the sliding set. Therefore, we will show that the flat periodic orbit of the linear system has quite different dynamics due to the interaction between its trajectory and the nonlinear sliding surface, and a set of such hidden trajectories.

If we assume that $\mathcal{X}_0 \in \tilde{\Sigma}^c_+$, then the general solution of this system is given by

$$\begin{aligned} x(t) &= x_0 \cos(\beta t) + y_0\alpha_1 \sin(\beta t)/\beta, \\ y(t) &= y_0 \cos(\beta t) - x_0\beta \sin(\beta t)/\alpha_1, \\ z(t) &= z_0 \exp(\alpha_3 t). \end{aligned} \tag{3.5}$$

The duration of time required for the trajectory to return to $\tilde{\Sigma}$ is given by finding the first positive solution to the following equation:

$$H(\mathcal{X}(t), \alpha) = \gamma_1 z(t) + \gamma_2 y(t) + \gamma_3 x(t)^3 = 0.$$

Mathematical software, such as Maple, can compute a series approximation of this equation, yielding the first positive approximate symbolic solution. Now, we consider a novel sub-system of (2.2) without an equilibrium point, which is described as:

$$\dot{\mathcal{X}} = F_1(\mathcal{X}, \alpha) = \begin{pmatrix} \alpha_4 z + \alpha_5 \\ \alpha_6 z \\ -z + \alpha_7(1 - x^2)y \end{pmatrix}. \tag{3.6}$$

It should be noted that the attractors formed purely by this system without equilibria fall into the category of hidden attractors (according to the definition given by [30]). If $\alpha_5 = 0$, the system (3.6) can have an infinite number of equilibria. In other words, system (3.6) has an infinite number of equilibrium points when $\alpha_5 = 0$, as shown below:

$$E = \{\mathcal{X} \in \mathbb{R}^3 \mid x = \pm 1, y \in \mathbb{R}, z = 0\},$$

or

$$E = \{\mathcal{X} \in \mathbb{R}^3 \mid x = \mathbb{R}, y = 0, z = 0\}.$$

Further, both subsystems (3.4) and (3.6) remain dissipative if $\alpha_3 < 0$.

If we assume that $\mathcal{X}_0 \in \tilde{\Sigma}^c_-$, then the general solution of this system is given by

$$\begin{aligned} x(t) &= (z_0 - z(t))\,\alpha_4 + (\ln z_0 - \ln z(t))\,\alpha_5 + x_0, \\ y(t) &= (z_0 - z(t))\,\alpha_6 + y_0, \end{aligned} \tag{3.7}$$

note that $\phi_1(\mathcal{X}, t)$ is the solution of the linear system ($z(t) = z_0 \exp(-t)$ such that $\alpha_7 = 0$), and the general solution of the nonlinear system (i.e., $\alpha_7 \neq 0$) is given as:

$$\Phi_1(\mathcal{X}, t) = \phi_1(\mathcal{X}, t) + \Omega(\mathcal{X}, t).$$

The expression $\Omega(\mathcal{X}, t) = \int_0^t \phi_1(\mathcal{X}, t - s)G(\mathcal{X}(s))ds$ can be expressed explicitly, but the resulting formulas are somewhat complex. In addition, numerical evaluation is used to determine the first positive solution for the time it takes for the trajectory to return to $\tilde{\Sigma}$.

Once any subsystem's solution reaches $\tilde{\Sigma}^s_-$, the sliding mode trajectory is numerically computed by solving Eq (2.3).

According to the semi-analytical analysis above, (3.5) and (3.7) fully determines the dynamic behaviors of the system when cross mode is considered. An explicit expression of $\tilde{\mathcal{P}}_i(\mathcal{X}), i = 1, 2$ is obtained using (3.5) and (3.7). However, it is necessary to confirm the presence of times $T_i, i = 1, 2$ when the flow (2.2) crosses the discontinuity surface, which are unknown. It is possible to select a convenient Poincarés map section to be the switching surface. Then, we can present the Poincaré map in a lower-dimensional manifold, i.e., $\tilde{\mathcal{P}}$ has a 2- dimensional manifold. In this context, we consider the first trajectory, which can intersect the crossing and sliding regions

$$\Psi(\mathcal{X}) = \tilde{\mathcal{P}}(\mathcal{X}) - \mathcal{X} - \xi = 0,$$

thus, it follows that; $D_{\mathcal{X}}\tilde{\mathcal{P}}(\mathcal{X}) - I \neq 0$.

Lemma 1. *Let $\mathcal{X} \in \tilde{\Sigma}$ and consider that the first trajectory is the linearized Poincaré map given by* (3.3) *(such that $m = 1$). Further, the map $\tilde{\mathcal{P}}(\mathcal{X}, \alpha)$ satisfies the following conditions:*

(1) $\tilde{\mathcal{P}}(\bar{\mathcal{X}}, \bar{\alpha}) = \bar{\mathcal{X}}$ *which means that* $\bar{\mathcal{X}}$ *is a fixed point of the map* $\tilde{\mathcal{P}}$.

(2) The Jacobian $D_{\mathcal{X}}\tilde{\mathcal{P}}(\bar{\mathcal{X}})$ *has eigenvalues* $\sigma_c(\bar{\alpha}) = -1$ *and* $\sigma_\ell(\bar{\alpha}), \ell = 1, 2$ *with* $|\sigma_\ell(\bar{\alpha})| \neq 1$.

(3) Assume that $\xi(\alpha)$ *be the curve of* $\tilde{\mathcal{P}}$ *fixed points near* $\xi(\bar{\alpha})$ *and* $\sigma_\ell(\alpha), \ell = 1, 2$, *are eigenvalues of matrix* $D_{\mathcal{X}}\tilde{\mathcal{P}}(\mathcal{X})|_{(\xi(\alpha))}$, *then we get* $\Lambda = D_\alpha \sigma_c(\alpha)|_{\bar{\alpha}} \neq 0$.

Then, using the implicit function theorem, there exists $\mathcal{X}(\alpha)$, *passing through* $\bar{\mathcal{X}}$ *at* $\bar{\alpha}$, *and a period-doubling bifurcation occurs at* $(\bar{\mathcal{X}}, \bar{\alpha})$.

There is a technique for constructing the criteria to predict an individual period-doubling bifurcation for the systems (3.4) and (3.6) that can be used with the Poincaré map. Without loss of generality, we assume that $\left(\bar{\mathcal{X}}, \bar{\alpha}\right) = (0, 0)$ is a fixed point of the Poincaré map $\tilde{\mathcal{P}}$ and $\mathcal{X}(\alpha) \in \tilde{\Sigma}$ is a bifurcation neighborhood of $\mathcal{X}(0) \in \tilde{\Sigma}$. Applying the implicit function theorem to $\mathcal{X}(\alpha)$, we can generate a "branch" of continuous solutions $\mathcal{X}$ with regard to the bifurcation parameter α defined in some region of $\alpha = 0$. This setting reduces the dimension of the discrete Poincaré map to one, allowing Li and Yorke's result to be applied to $\tilde{\mathcal{P}}$, for more details, see [31, 32]. In this context, the following conditions are required in order to predict chaotic behavior using the period-doubling method performed on the corresponding Poincaré map: We determine for the map $\tilde{\mathcal{P}}$, three distinct points, such that $\tilde{\mathcal{P}}(\mathcal{X}) = \xi$, $\tilde{\mathcal{P}}(\xi) = \eta$ and $\tilde{\mathcal{P}}(\eta) = \mathcal{X}$, $\mathcal{X} \neq \xi \neq \eta$. Thus, under assumption 1 in Lemma 1, it is equivalent to (i) $\Omega = D_{\mathcal{X}}\tilde{\mathcal{P}}(\mathcal{X}) - 1 \neq 0$, (ii) $\Omega\tilde{\Omega} - 1 \neq 0$ and (iii) $\Omega\tilde{\Omega}\tilde{\tilde{\Omega}} - 1 \neq 0$, such that $\tilde{\Omega} = -(D_{\mathcal{X}}\tilde{\mathcal{P}}(\mathcal{X}) - 1)^{-1}$, $\tilde{\tilde{\Omega}} = -(\Omega\tilde{\Omega} - 1)^{-1}$.

4. Results and discussion

To advance the study of our system, we discuss the influence of various parameters of interest on flow behavior using numerical analysis. The above analytical results are used to investigate the properties of the system that are dependent on parameters and to identify relevant parameters' ranges.

Simply modify the control parameter α_3 and keep the other parameters constant as follows: $\alpha_1 = 0.322, a = 1.3, \alpha_2 = -1.58, \alpha_4 = 2.30, \alpha_5 = 1.70; \alpha_6 = 3.49, \alpha_7 = 3.24a$, $\gamma_1 = -\gamma_2 = \gamma_3 = -1$. We show that at $\alpha_3 = -0.2$, the system has only a single periodic orbit involving sliding mode which is illustrated in (Figure 2(a),(b)). By varying α_3 from -0.11 to -0.1 to -0.011, we observe period-doubling, period-4 orbit, and chaotic behavior (Figure 2(c)–(h)), respectively.

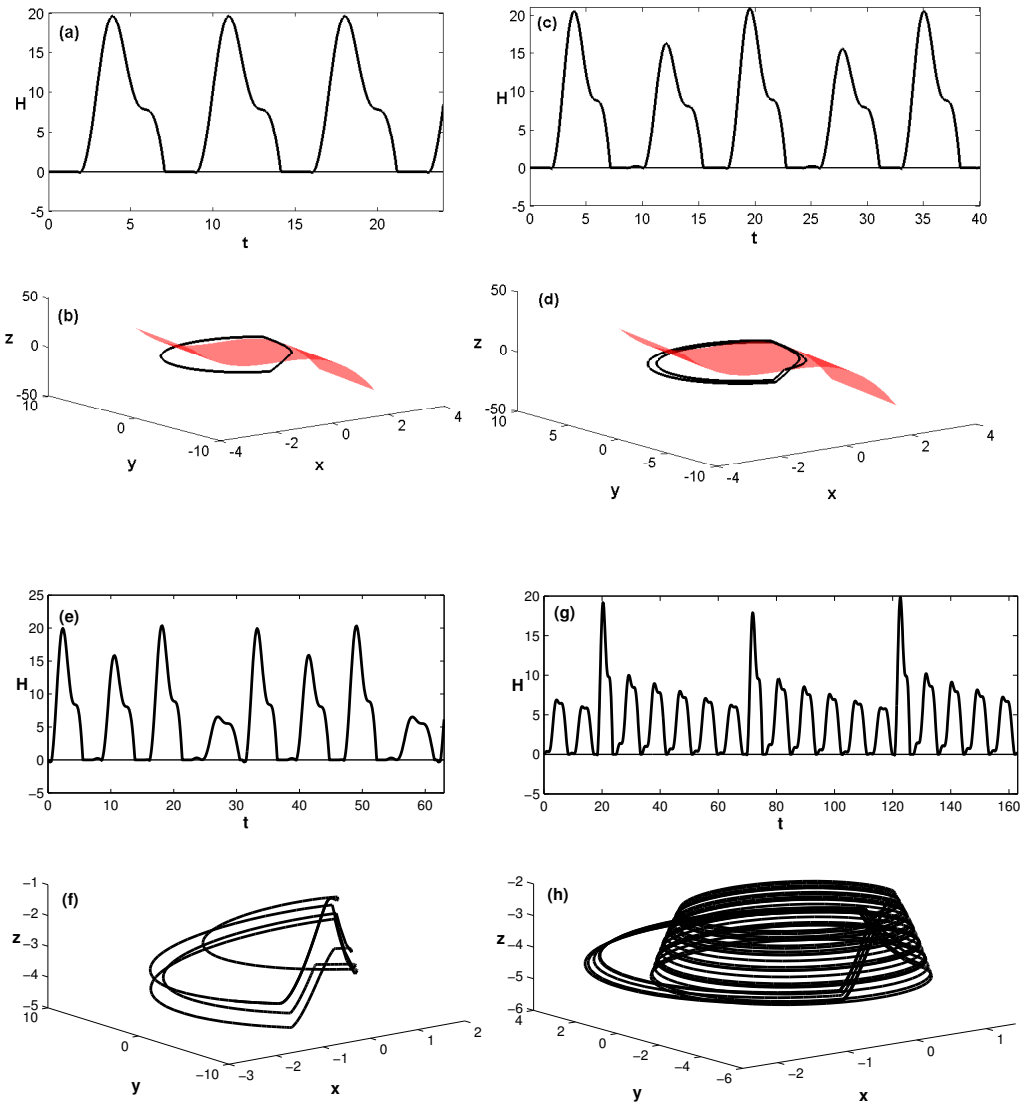

Figure 2. Numerical simulations of subsystems (3.4) and (3.6) for varying values of α_3. Figure (a),(b) at $\alpha_3 = -0.2$, demonstrating single periodic orbit. Figure (c),(d) at $\alpha_3 = -0.11$, demonstrating period-doubling orbits. Figure (e),(f) at $\alpha_3 = -0.1$ demonstrating period-4 orbits. Figure (g),(h) at $\alpha_3 = -0.011$ demonstrating chaotic behavior.

To explore the effect of varying parameter α_1, we keep the other parameters constant as follows: $\alpha_2 = -1.0, \alpha_3 = -0.1, \alpha_4 = 2.30, \alpha_5 = 1.56, \alpha_6 = 2.6, \alpha_7 = 3.24a$, and $\gamma_1 = -\gamma_2 = \gamma_3 = -1$. Figure 3 shows that by varying the parameter α_1, the sliding period-doubling occurs at $\alpha_1 = 0.402$, presenting a route to sliding chaos at $\alpha_1 = 0.385$.

The sliding hypersurface can change position by changing one or more parameters $\gamma_i, i = 1, 2, 3$, resulting in a transition from a unique periodic orbit to a period-doubling orbit and giving birth to a period-4 orbit. For example, if the parameter γ_3 is varied and the other parameters are constant, as follows: $\gamma_1 = \gamma_2 = 1, \alpha_1 = 0.385; \alpha_2 = -1.0; \alpha_3 = -0.01, \alpha_4 = 2.30, \alpha_5 = 1.56, \alpha_6 = 2.6, \alpha_7 = 3.24a$. If $0.5 \leq \gamma_3 \leq 0.9$, our system shows rich dynamical behavior. At $\gamma_3 = 0.811$, Figure 4(a),(b) shows that

the system has a unique periodic orbit. When γ_3 slightly decreases beyond $\gamma_3 = 0.611$, the periodic orbit is destroyed and emerges a period-doubling orbit; see Figure 4(c),(d). Further at $\gamma_3 = 0.511$, the period-doubling orbit modifies to a period-4 orbit; see Figure 4(e),(f).

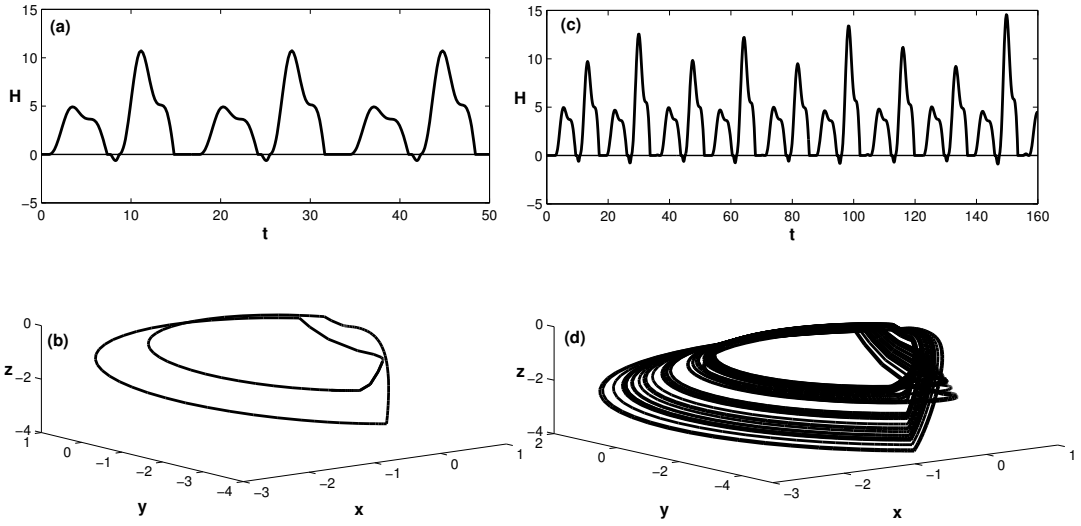

Figure 3. The system establishes a sliding period doubling orbit at $\alpha_1 = 0.402$ (Figure 3(a),(b)), presenting a path to chaos at $\alpha_1 = 0.385$ (Figure 3(c),(d)).

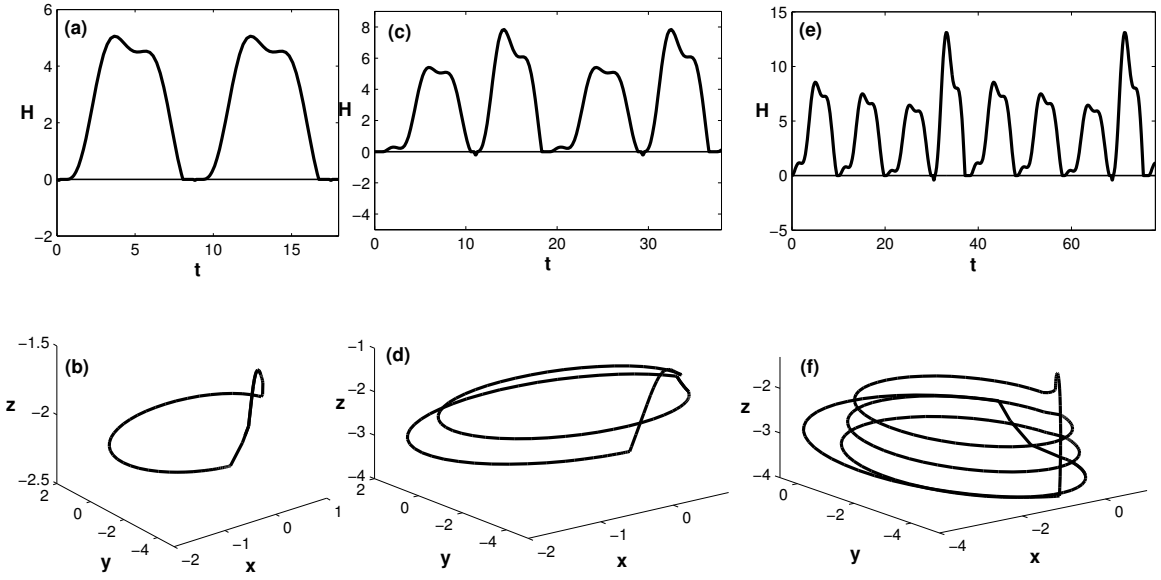

Figure 4. A shifting hypersurface results in (a),(b) a unique periodic orbit at $\gamma_3 = 0.811$. (c),(d) Period-doubling orbit at $\gamma_3 = 0.611$. (e),(f) Period-4 orbit at $\gamma_3 = 0.511$.

According to Figure 5, the behavior of the system undergoes a rich dynamical behavior as the parameter α_2 varies while the other parameters, $\alpha_1 = 0.385, \alpha_3 = -0.3, \alpha_4 = 2.30, \alpha_5 = 1.56, \alpha_6 = 2.6, \alpha_7 = 3.216a$, remain constant. The system initially displays periodic solutions ((a) at $\alpha_2 = -1.0$) that transform into period-doubling orbits ((b) $\alpha_2 = -1.1$), then period-3 orbits ((c) at $\alpha_2 = -1.15$), and eventually generates a chaotic attractor involving a sliding mode close to the hypersurface ((d) at $\alpha_2 = -1.17$).

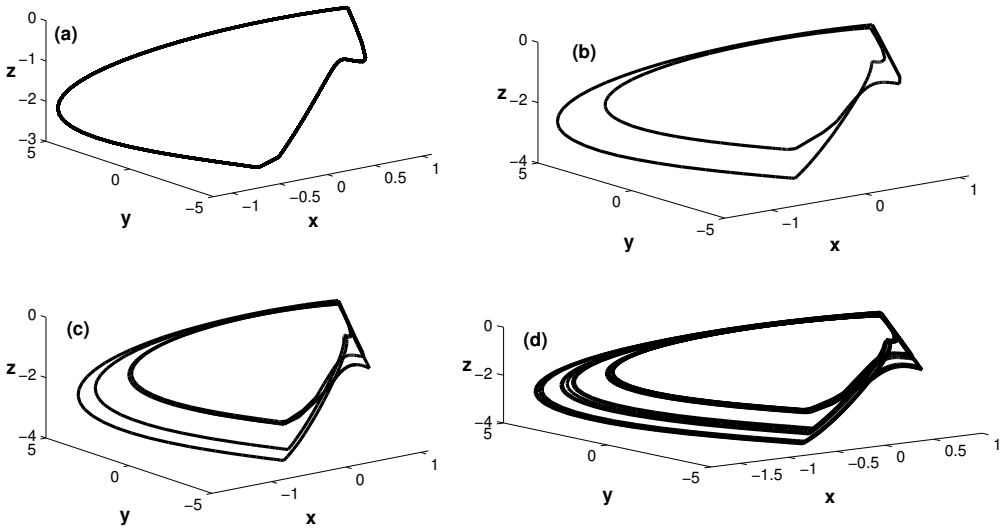

Figure 5. Varying the parameter α_2 results in (a) a unique periodic orbit at $\alpha_2 = -1.0$. (b) Period-doubling orbit at $\alpha_2 = -1.1$. (c), Period-3 orbits at $\alpha_2 = -1.15$. (d) chaotic attractor involving a sliding mode at $\alpha_2 = -1.17$.

To support the verification of period-m orbit and chaos in the discontinuous system with infinite equilibria. Set $\alpha_5 = 0$ and $\alpha_1 = 0.2, \alpha_2 = -0.17, \alpha_3 = -0.2, \alpha_6 = 1.8, \alpha_7 = 3.216a$ while varying the value of α_4. Because the subsystem (3.6) has an infinite number of equilibrium points, its hidden trajectories are preserved. Figure 6 shows the route from period-m orbit with $\alpha_1 = 0.67$ to chaos with $\alpha_4 = 0.7$, (see Figure 6).

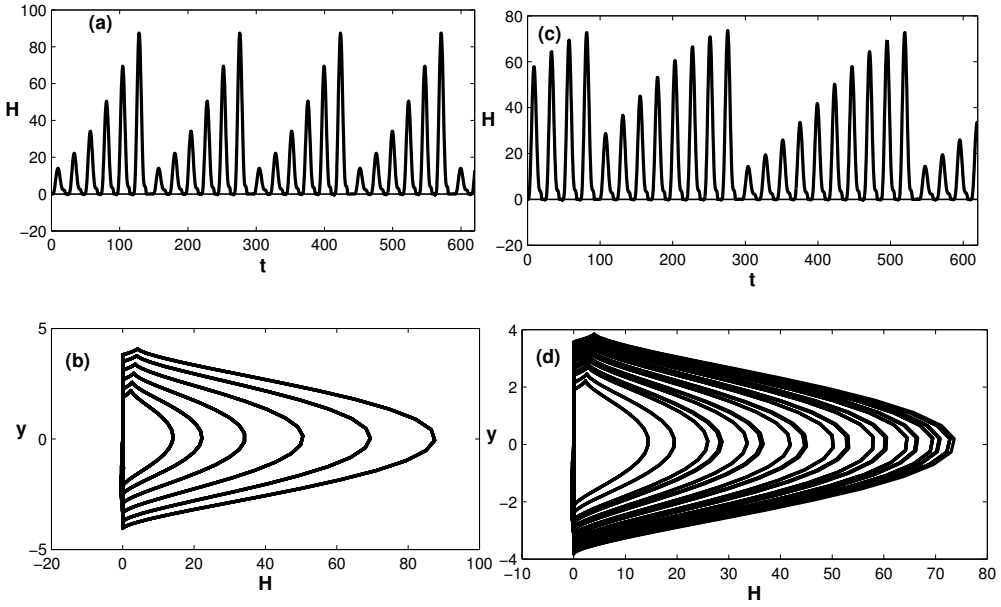

Figure 6. Period-m orbit and chaotic attractor of the discontinuous system when the subsystem (3.6) has infinite equilibria. (a),(b) a period-6 orbit involving a sliding mode at $\alpha_4 = 0.67$. (c),(d) chaotic attractor involving a sliding mode at $\alpha_4 = 0.7$.

5. Conclusions

In this paper, we have presented a mathematical analysis of the trajectory leading to sliding period doubling and chaotic dynamics in a novel, simple discontinuous system with a three-dimensional configuration that incorporates a sliding surface. We proposed a switching system composed of dissipative subsystems, one of which is linear and the other not associated with equilibria. The explicit solutions for each subsystem have been obtained and used to establish the Poincaré return map. By varying the linear system's parameters, it has been shown that the sliding period-m orbit emerged, resulting in the emergence of chaos from a previously single period one. It has been observed that, due to the presence of a nonlinear sliding surface and a set of such hidden trajectories, the system exhibits varied dynamic responses ranging from periodic to chaotic.

Author contributions

Hany A. Hosham and Thoraya N. Alharthi: Writing – review and editing. All authors have read and agreed to the published version of the manuscript.

Use of AI tools declaration

The authors declare they have not used Artificial Intelligence (AI) tools in the creation of this article.

Acknowledgments

The authors are thankful to the Deanship of Graduate Studies and Scientific Research at University of Bisha for supporting this work through the Fast-Track Research Support Program.

Conflict of interest

The authors declare no conflict of interest in this paper.

References

1. M. Bernardo, C. Budd, A. R. Champneys, P. Kowalczyk, *Piecewise-smooth dynamical systems: Theory and applications*, Springer Science Business Media, **163** (2008).
2. D. Weiss, T. Küpper, H. A. Hosham, Invariant manifolds for nonsmooth systems, *Physica D*, **241** (2012), 1895–1902. https://doi.org/10.1016/j.physd.2011.07.012
3. N. Guglielmi, E. Hairer, Sliding modes of high codimension in piecewise-smooth dynamical systems, *Numer. Algorithms*, **94** (2023), 257–273. https://doi.org/10.1007/s11075-023-01499-9
4. V. Avrutin, M. R. Jeffrey, Bifurcations of hidden orbits in discontinuous maps, *Nonlinearity*, **34** (2021), 6140–6172. https://doi.org/10.1088/1361-6544/ac12ac
5. M. R. Jeffrey, *Hidden dynamics: The mathematics of switches, decisions and other discontinuous behaviour*, Springer, 2018.
6. H. F. Han, S. L. Li, Q. S. Bi, Non-smooth dynamic behaviors as well as the generation mechanisms in a modified Filippov-type Chua's circuit with a low-frequency external excitation, *Mathematics*, **10** (2022), https://doi.org/10.3390/math10193613
7. F. Luo, Y. D. Li, Y. Xiang, Bifurcation of limit cycles from a focus-parabolic-type critical point in piecewise smooth cubic systems, *Mathematics*, **12** (2024), 702. https://doi.org/10.3390/math12050702
8. H. A. Hosham, Discontinuous phenomena in bioreactor and membrane reactor systems, *Int. J. Biomath.*, **12** (2019). https://doi.org/10.1142/S1793524519500463
9. M. Pasquini, D. Angeli, On convergence for hybrid models of gene regulatory networks under polytopic uncertainties: A Lyapunov approach, *J. Math. Biol.*, **83** (2021). https://doi.org/10.1007/s00285-021-01690-3
10. S. F. Luo, D. S. Wang, W. X. Li, Dynamic analysis of a SIV Filippov system with media coverage and protective measures, *AIMS Math.*, **7** (2022), 13469–13492. https://doi.org/10.3934/math.2022745
11. H. J. Peng, C. C. Xiang, A Filippov tumor-immune system with antigenicity, *AIMS Math.*, **8** (2023), 19699–19718. https://doi.org/10.3934/math.20231004
12. A. Pisano, E. Usai, Sliding mode control: A survey with applications in math, *Math. Comput. Simul.*, **81** (2011), 954–979. https://doi.org/10.1016/j.matcom.2010.10.003
13. J. Awrejcewicz, M. Fečkan, P. Olejnik, Bifurcations of planar sliding homoclinics, *Math. Probl. Eng.*, **2006** (2006), 1–13. https://doi.org/10.1155/MPE/2006/85349

14. H. A. Hosham, Bifurcation of periodic orbits in discontinuous systems, *Nonlinear Dyn.*, **87** (2017), 135–148. https://doi.org/10.1007/s11071-016-3031-7

15. D. Weiss, T. Küpper, H. A. Hosham, Invariant manifolds for nonsmooth systems with sliding mode, *Math. Comput. Simul.*, **110** (2015), 15–32. https://doi.org/10.1016/j.matcom.2014.02.004

16. M. Balcerzak, A. Dabrowski, B. Blazejczyk-Okolewska, A. Stefanski, Determining Lyapunov exponents of non-smooth systems: Perturbation vectors approach, *Mech. Syst. Signal Process.*, **141** (2020), 106734. https://doi.org/10.1016/j.ymssp.2020.106734

17. Z. Zhang, Y. Liu, J. Sieber, Calculating the Lyapunov exponents of a piecewise-smooth soft impacting system with a time-delayed feedback controller, *Commun. Nonlinear Sci. Numer. Simul.*, **91** (2020), 105451. https://doi.org/10.1016/j.cnsns.2020.105451

18. G. S. Vicinansa, D, Liberzon. Estimation entropy, Lyapunov exponents, and quantizer design for switched linear systems, *SIAM J. Control Optim.*, **61** (2023), 198–224. https://doi.org/10.1137/21M1411871

19. M. Feckan, M. Pospíšil, *Poincaré-Andronov-Melnikov analysis for non-smooth systems*, Academic Press, 2016.

20. S. Wiggins, D. S. Mazel, Introduction to applied nonlinear dynamical systems and chaos, 1990.

21. N. Kuznetsov, T. Mokaev, V. Ponomarenko, E. Seleznev, N. Stankevich, L. Chua, Hidden attractors in Chua circuit: Mathematical theory meets physical experiments, *Nonlinear Dyn.*, **111** (2023), 5859–5887. https://doi.org/10.1007/s11071-022-08078-y

22. J. Llibre, M. A. Teixeira, Piecewise linear differential systems without equilibria produce limit cycles? *Nonlinear Dyn.*, **88** (2017), 157–164.

23. Z. K. Li, X. B. Liu, Limit cycles in discontinuous piecewise linear planar Hamiltonian systems without equilibrium points, *Int. J. Bifurc. Chaos*, 2022. https://doi.org/10.1142/S021812742250153X

24. M. R. Jeffrey, A. Colombo, The two-fold singularity of discontinuous vector fields, *SIAM J. Appl. Dyn. Syst.*, **8** (2009), 624–640. https://doi.org/10.1137/08073113X

25. R. Cristiano, B. R. De Freitas, J. C. Medrado, Three crossing limit cycles in a 3D-Filippov system having a T-singularity, *Int. J. Bifurc. Chaos*, **32** (2022). https://doi.org/10.1142/S0218127422500067

26. B. R. Hunt, J. A. Kennedy, T. Y. Li, H. E. Nusse, *The theory of chaotic attractors*, Springer Science Business Media, 2004.

27. L. Dieci, L. Lopez, Fundamental matrix solutions of piecewise smooth differential systems, *Math. Comput. Simul.*, **81** (2011), 932–953. https://doi.org/10.1016/j.matcom.2010.10.012

28. H. A. Hosham, Bifurcation of limit cycles in piecewise-smooth systems with intersecting discontinuity surfaces, *Nonlinear Dyn.*, **99** (2020), 2049–2063. https://doi.org/10.1007/s11071-019-05400-z

29. H. A. Hosham, Nonlinear behavior of a novel switching jerk system, *Int. J. Bifurc. Chaos*, **30** (2020).

30. G. A. Leonov, N. V. Kuznetsov, V. I. Vagaitsev, Localization of hidden Chuas attractors, *Phys. Lett. Sect. A Gen. At. Solid State Phys.*, **375** (2011), 2230–2233.

31. D. Benmerzouk, J. P. Barbot, Chaotic behavior analysis based on sliding bifurcations, *Nonlinear Anal. Hybrid Syst.*, **4** (2010), 503–512. https://doi.org/10.1016/j.nahs.2009.12.001

32. D. Benmerzouk, J. P. Barbot, Symmetries impact in chaotification of piecewise smooth systems, *Nonlinear Dyn. Syst. Theory*, **16** (2016), 149–164.

AIMS Press